


The tracheal system in post-embryonic development of holometabolous insects: a case study using the mealworm beetle

Marcin Raś,  Dariusz Iwan and Marcin Jan Kamiński

Zoological Museum, Museum and Institute of Zoology, Polish Academy of Sciences, Warsaw, Poland

Abstract

The tracheal (respiratory) system is regarded as one of the key elements which enabled insects to conquer terrestrial habitats and, as a result, achieve extreme species diversity. Despite this fact, anatomical data concerning this biological system is relatively scarce, especially in an ontogenetic context. The purpose of this study is to provide novel and reliable information on the post-embryonic development of the tracheal system of holometabolous insects using micro-computed tomography methods. Data concerning the structure of the respiratory system acquired from different developmental stages (larvae, pupae and adults) of a single insect species (*Tenebrio molitor*) are co-analysed in detail. Anatomy of the tracheal system is presented. Sample sizes used (29 individuals) enabled statistical analysis of the results obtained. The following aspects have been investigated (among others): the spiracle arrangement, the number of tracheal ramifications originating from particular spiracles, the diameter of longitudinal trunks, tracheal system volumes, tracheae diameter distribution and fractal dimension analysis. Based on the data acquired, the modularity of the tracheal system is postulated. Using anatomical and functional factors, the following respiratory module types have been distinguished: cephalo-prothoracic, metathoracic and abdominal. These modules can be unambiguously identified in all of the studied developmental stages. A cephalo-prothoracic module aerates organs located in the head capsule, prothorax and additionally prolegs. It is characterised by relatively thick longitudinal trunks and originates in the first thoracic spiracle pair. Thoracic modules support the flight muscles, wings, elytra, meso- and metalegs. The unique feature of this module is the presence of additional longitudinal connections between the neighbouring spiracles. These modules are concentrated around the second prothoracic and the first abdominal spiracle pairs. An abdominal module is characterised by relatively thin ventral longitudinal trunks. Its main role is to support systems located in the abdomen; however, its long visceral tracheae aerate organs situated medially from the flight muscles. Analysis of changes of the tracheal system volume enabled the calculation of growth scaling among body tissues and the volume of the tracheal system. The data presented show that the development of the body volume and tracheal system is not linear in holometabola due to the occurrence of the pupal stage causing a decrease in body volume in the imago and at the same time influencing high growth rates of the tracheal system during metamorphosis, exceeding that ones observed for hemimetabola.

Key words: endopterygota; holometabola; insects; metamorphosis; microtomography; respiratory system; tracheal system.

Introduction

Holometabolous insects (Endopterygota) are a morphologically and ecologically diverse worldwide radiation of over 850 000 described species (Grimaldi & Engel, 2005; Beutel &

Pohl, 2006), with many more still awaiting discovery (May, 2011; Mora et al. 2011). Among others, this taxon is represented by such mega-diverse insects groups as beetles, flies, moths and bees. It is believed that the occurrence of the pupal stage in the life cycle of Endopterygota is the main adaptation that has had the most significant effect on the evolution of this clade (Nicholson et al. 2014; Ferns & Jervis, 2016). However, general understanding of the origin and the exact role of this unique stadium, especially in an ontogenetic context, remains unsatisfactory (Ebenman, 1992; Haug et al. 2015; Ureña et al. 2016).

Correspondence

Marcin Raś, Zoological Museum, Museum and Institute of Zoology, Polish Academy of Sciences, ul. Wilcza 64, 00-679 Warsaw, Poland.
E: mras@miiz.waw.pl

Accepted for publication 22 February 2018
Article published online 24 March 2018

The tracheal (respiratory) system is one of the key features that enabled insects to conquer terrestrial habitats and as a result achieve extreme species diversity (Bradley et al. 2009). The tube-based respiratory systems probably arose independently several times among arthropods (i.e. Hexapoda, Myriapoda, Arachnida) (Kraus, 1997; Grimaldi, 2010); however, the tracheal system of Endopterygota seems to be homologous (Tonapi, 1977). The respiratory system of holometabolous insects comprises a network of gas-filled, cuticle-lined tubes (tracheae and tracheoles) located inside the body, which exchange respiratory gases between the tissues and the environment (e.g. Tonapi, 1977; Lowe et al. 2013; Iwan et al. 2015). It is connected to the atmosphere by spiracles, which lie laterally on body segments. In more detail, spiracles consist of peritreme that surrounds the atrial orifice, behind which the atrium lies. The closing apparatus, which separates the spiracles from the tracheae, is located on the bottom of the atrium (Snodgrass, 1935). The number of spiracles can vary depending on species or even stages of life (Snodgrass, 1935; Lawrence et al. 1994, 2011; Gillott, 2005; Duncan et al. 2010); however, a holoneustic arrangement (10 pairs) is believed to be the most primitive (Richards & Davies, 1977). Opening and closing of spiracles is controlled by muscles that are driven by impulses from the ventral nerve cord.

During ontogenesis, the tracheal system originates from the ectoderm (Casanova, 2007). It arises in the embryonic stage as an invagination of 10 pairs of sacs composed of approximately 80 cells each (Pitsouli & Perrimon, 2010). This developmental phase is mainly regulated by the expression of the tracheless (*trh*) gene, which encodes the bHLH-PAS transcription factor (Long et al. 2014). Subsequently, some of the cell buds from the tracheal sacs in different directions form the main tracheal branches, which successively sprout secondary and terminal ramifications (Affolter & Shilo, 2000). Whereas morphogenesis of the primary trachea is strictly controlled by genetic drivers, which results in relative structural invariability of this part of the tracheal system (Pereanu et al. 2007), the development of secondary and higher order branches (including tracheoles) is more influenced by other factors (e.g. hypoxia) (Wigglesworth, 1954; Centanin et al. 2010). Nevertheless, ontogenesis of the tracheal system is regulated by a complex network of genes (e.g. branchless, breathless, knickkopf, membrin, polychaetoid, TSG101, wingless, whacked) (Sutherland et al. 1996; Metzger & Krasnow, 1999; Ghabrial et al. 2011; Long et al. 2014).

Although the phenomenon of gas exchange is one of the major research trends in insect physiology (Greenlee & Harrison, 2005; Harrison et al. 2005; Jögar et al. 2005; Lease et al. 2006; Greenlee et al. 2009; Contreras & Bradley, 2010; Moerbitz & Hetz, 2010; Nespolo et al. 2011; Sláma & Jedlička, 2012), the structure of the tracheal system remains poorly investigated. Earlier works addressing this issue were based on dissections and illustrated with

handmade drawings (e.g. Packard, 1898; Whitten, 1957; Hafeez & Gardiner, 1964; Tonapi, 1977), and are therefore prone to artefacts. For instance, Crowson (1981) states that beetle larval instars are equipped with a single primary order thoracic trachea on each side, as in the abdomen, which is not consistent with the most recent findings (Iwan et al. 2015). This kind of oversight may have great implications for studies concerning physiology of gas exchange. Additionally, more detailed descriptions of the tracheal system were restricted to certain body parts, such as the head capsule or legs (Locke, 1958; Romer, 1971), and the anatomy of other elements, such as the wings and their homologues, have consistently been neglected (e.g. Hafeez & Gardiner, 1964; however, see Chapman, 1918). Furthermore, in an ontological context, the structure of the tracheal systems in the different life stages of a single species were described separately, often by different authors – this is the case for both hemi- and holometabolous insects (e.g. Scott, 1905; Snodgrass, 1910; Kennedy, 1922; Given, 1944). Finally, there is little available data on morphometric changes of the tracheal system during post-embryonic development (for hemimetabola see Harrison et al. 2005; Lease et al. 2006).

The structure of a tracheal system significantly changes through post-embryonic development (Whitten, 1957; Lowe et al. 2013; Iwan et al. 2015). Functional modifications are introduced during each ecdysis (Loudon, 1989; Callier & Nijhout, 2011; Helm & Davidowitz, 2013). The new tracheal system is built around the old one during the preceding instar and is fully developed by the time of ecdysis (Locke, 1958; Snelling et al. 2011). It starts delivering respiratory gases immediately after the shedding of the old cuticle. According to the generalised model described for holometabolous insects, the basic larval pattern of the tracheal system is taken through the larval stadium to the imago, with drastic changes occurring only in the thorax where the flight muscles and wings develop (Keister, 1948; Whitten, 1968). Although this model was proposed for flies, it can be also applied to beetles (Iwan et al. 2015). Another scheme of post-embryonic development of the tracheal system was described for the fruit fly (*Drosophila melanogaster*) (Whitten, 1957). In this case, during the larva–pupa transition the posterior half of the already existing system is histolysed and subsequently formed *de novo* in the pupal stadium (Whitten, 1957). However, this type of tracheal system development seems to be less common than the first one (see also Nardi & Ujhelyi, 1998).

Recently, a new era in tracheal system research was initiated by the development of micro-computed tomography (μ CT) (Kaiser et al. 2007; Socha et al. 2008, 2010; Greenlee et al. 2013; Lowe et al. 2013; Waters et al. 2013; Greco et al. 2014; Iwan et al. 2015). Thanks to this approach, the respiratory system and other body parts can be visualised in three dimensions without any risk of deformation by direct

manipulation (Westneat et al. 2008; Li et al. 2011; Walker et al. 2014; Smith et al. 2016). Moreover, μ CT enables exact measurements of the features of the tracheal system, including its total volume or diameters of the particular tracheae etc. (e.g. Kaiser et al. 2007). Potential advantages and limitations of this method in this context were discussed by Iwan et al. (2015), who concluded that this method seems to be a suitable tool for comprehensive analyses of tracheal system, including its developmental aspect. However, the application of this method to this field has not yet reached its full potential.

Adults of *Tenebrio molitor* L. represent the basic morphological bauplan of Coleoptera (Crowson, 1955; Doyen, 1966). *Tenebrio molitor* has two pairs of wings, the first of which is modified into elytra, while the second pair is used for active flight and is hidden under the elytra during rest or pedal locomotion. Before pupation, *T. molitor* undergoes over a dozen larval instars (Morales-Ramos et al. 2015), which are morphologically similar and differ mostly in body size. The pupa of *T. molitor* is of the exarate type, which means that its appendages (legs, antennae and wing rudiments) lie free and are not soldered to the body. The structure of the tracheal system of this species was studied by a few authors (Table 1), but the available data remains far from complete. The general arrangement of the main trachea suggests that the *T. molitor* may be treated as a reference model for majority of Endopterygota (Whitten, 1968).

The purpose of this study was to provide novel and reliable data on the post-embryonic ontogeny of the tracheal system of holometabolous insects using a model organism (*T. molitor*) and μ CT methods. Data concerning the structure of respiratory system acquired from different developmental stages (larvae, pupae and adults) of *T. molitor* is co-analysed in detail. The dynamics of the tracheal system modifications throughout metamorphosis was modelled and illustrated. Based on topological, developmental and functional criteria, a new nomenclature of particular tracheae of the insects' respiratory system is proposed. The results presented here provide a hitherto unavailable background for various other kinds of research, including gas exchange physiology.

Materials and methods

Insect preparation

All specimens of *T. molitor* were reared at room temperature (~ 22.0 °C) with full access to food (oatmeal, bread, flour). Ten specimens representing each post-embryonic developmental stage (older instar larvae, pupae and adults) were randomly selected for further analysis. However, due to some technical difficulties during the scanning process, only 29 models (10 larvae, 10 adults and nine pupae) were obtained. Selected 3D models are provided in the supplementary information to this publication (Raś, 2017: S1–4). Prior to scanning, individuals were frozen (-20.0 °C) and then stored in a refrigerator or mounted in a pipette tip or an Eppendorf tube and processed immediately with the μ CT system (for details see Iwan et al. 2015). The reference material, preserved in 70% ethanol, was deposited at the entomological collection of the Museum and Institute of Zoology (Polish Academy of Science, Warsaw, Poland).

Additionally, to study the relationships between selected internal organs (central nervous system, muscles, digestive system) and the tracheal system, two of the above-mentioned adult individuals were rescanned after application of CPD (critical point drying) preparation and procedure, that is, these specimens were fixed in 4% buffered formalin and 2% glutaraldehyde solution prior to transferring through an ascending alcohol series (35, 50, 75, 96%). Samples were dried using an E3100 Critical Point Dryer (Quorum Technologies).

MicroCT system and scanning process

X-ray microtomographic analyses were performed at the Museum and Institute of Zoology of the Polish Academy of Sciences using a μ CT SkyScan 1172 system (SkyScan 2005). During the scanning processes, the X-ray source was set to a voltage of 40 kV and a current of 250 mA. Images were obtained using two binning modes: no binning and 2×2 . Due to their specific body shape, the larvae were scanned using five to seven oversized scans, and three to four oversized scans were performed on the pupae and adults (Iwan et al. 2015).

Reconstruction was performed using NREACON software (version 1.6.4.7) and the tracheal system segmentation process was conducted in CTAN (version 1.11.10) using the method proposed by Iwan et al. (2015) (semiautomatic approach). The final resolution of the models obtained ranged from 6.3 to 7.7 μ m per pixel and thus, to avoid artefacts, the minimal diameter of a single trachea in –2023574822 the trachea diameter distribution –2023574822 analysis in all investigated distributional stages was set to 25.0 μ m (Fig. 1B). What is more, for closer examination of a teratology discovered in the tracheal system of the antennae of a single adult

Table 1 List of available publications concerning the structure of *Tenebrio molitor* tracheal system.

References	Method	Studied stadium	Analysed aspects of the tracheal system
Romer (1971)	Manual dissection	Larva	Head and prothoracic trachea
Loudon (1989)	Manual dissection	Larva	Spiracles with main tracheae; diameter measurements
Kaiser et al. (2007)	Synchrotron	Imago	Tomograms of the whole insect; diameter measurements of head and leg tracheae; estimation of tracheal system volume
Iwan et al. (2015)	Micro-CT	Larva, pupa, imago	Three-dimensional models of the whole tracheal system; estimation of tracheal system volume

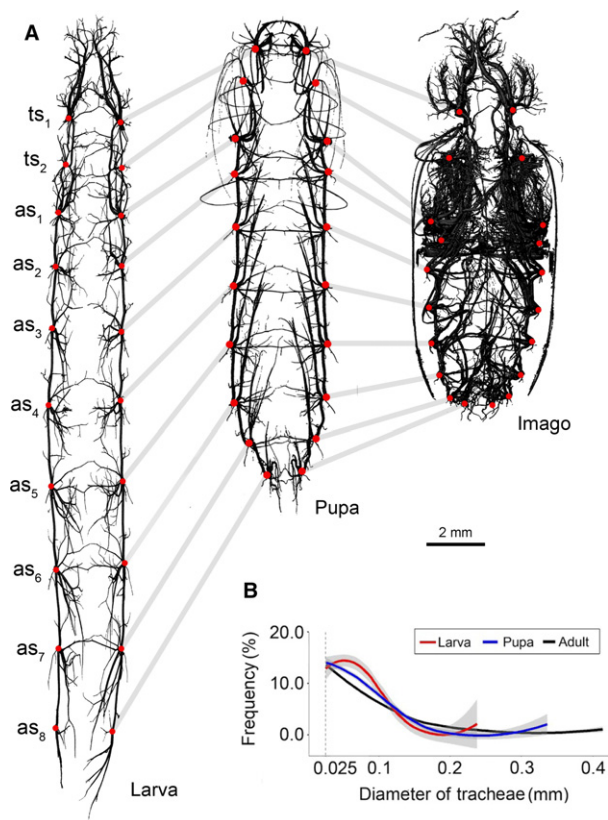


Fig. 1 Anatomy of the tracheal system and trachea thickness distribution in studied developmental stages of *Tenebrio molitor*. (A) Three-dimensional models of the respiratory system of larva, pupa and imago (dorsal views). Red dots indicate the placement of spiracles and tracheal vestibules. (B) Loess curves fitted to the scatterplots for trachea diameter distribution in different developmental stages. Lines correspond to percentage of whole tracheal system volume occupied by trachea of given diameter; grey region indicates standard error. as1–as8, spiracles of abdominal segments 1–8; ts1, mesothoracic spiracle; ts2, metathoracic spiracle.

specimen, the head capsule and prothorax of this individual were disarticulated and rescanned closer to the X-ray source to obtain a more detailed model (Fig. 2D).

Measurements, visualisation and statistical analysis

The analysis of the tracheal system topology and model optimisation was performed using BLENDER software (version 2.77) on datasets converted into stereolithography (STL) format. The distances between spiracle centres and longitudinal tracheae diameters were measured using DATAVIEWER software (version 1.4.4). The lengths between spiracles were measured in a 3D environment by placing markers in the centre of spiracles (marking the shortest path).

Measurements of visceral tracheae lengths and tracheal vestibules volumes were taken in NEUROMORPH extension to BLENDER software (Jorstad et al. 2014). Visceral tracheae lengths were measured using the 'shortest distance method', which creates a curve that runs on a model surface following the shortest distance between two data points. The direction of each visceral trachea was evaluated based on its longest branch. Volumes of tracheal vestibules

were measured via manual marking of vertices belonging to a particular vestibule and using the 'volume' option. Volumes of the whole tracheal systems, insects' bodies and fractal dimension were analysed in CTAN. The results of the subsequent analysis were visualised in CTVOX program (version 3.2.0).

Tracheal thickness distribution (Hildebrand & Rügsegger, 1997) analysis was performed in CTAN software using an algorithm which primarily designates a curve running centrally through the object of analysis (the skeletonisation process) and then builds up a series of spheres based on the path obtained previously (the sphere-fitting process). The spheres must meet the following criteria: the centre of a given sphere is located on the curve designated in the skeletonisation process and the outer layer of a given sphere is limited by the external surface of the analysed object. Based on the results obtained, the average tracheal thickness distribution values were calculated for each developmental stage analysed (Fig. 1B).

The following statistical analyses were performed using R software (version 3.2.3) (R Core Team 2013). Analysis of variance (ANOVA) and Tukey's Honest Significant Difference tests were used to identify significant contrasts between particular metric features of analysed structures, i.e. differences in diameter of major longitudinal tracheae trunks (Fig. 3A), to investigate tracheal vestibules volume to the whole body volume ratio (Figs 3B and 4), the distance between the spiracles of a given pair to the head capsule width ratio (Fig. 3C), the distance between the spiracles of the neighbouring body segments to the total body length ratio (Fig. 3D) and tracheal system volume differences between analysed developmental stages (Table 2). Level of significance was set to $\alpha = 0.05$.

To analyse the relation between volumes of the whole tracheal system and the whole body, a standardised major axis (SMA) method was used. Calculations were made in SMATR 3 package (Warton et al. 2012) after logarithmic transformation of analysed data. The differences between local regression curves fitted to the scatterplots for the tracheae diameter distribution were evaluated with a non-parametric, two-sample Kolmogorov–Smirnov test procedure (Sokal & Rohlf, 2011). The results of the above-mentioned statistical analyses were visualised using the GGPLOT2 package (Wickham, 2009). Raw data are available the supplementary information (Raś, 2017: S5–10).

The input data for the performed analyses and all three-dimensional models obtained here are accessible from the Harvard Dataverse repository (see Raś, 2017).

Terminology

One of the goals of this paper was to introduce a new nomenclature for particular tracheae of the insect respiratory system; however, rather than starting *de novo*, the authors used and further developed terminological systems proposed by Crowson (1981), Hafeez & Gardiner (1964), and Whitten (1957, 1968). Nomenclature of other morphological and anatomical structures follows that of Doyen (1966). Special terminology was used for the muscular system (see Beutel & Komarek, 2004).

Results

Topology

Tracheal system terminology

Detailed investigation of the obtained 3D models led to the identification of some key elements of the tracheal system

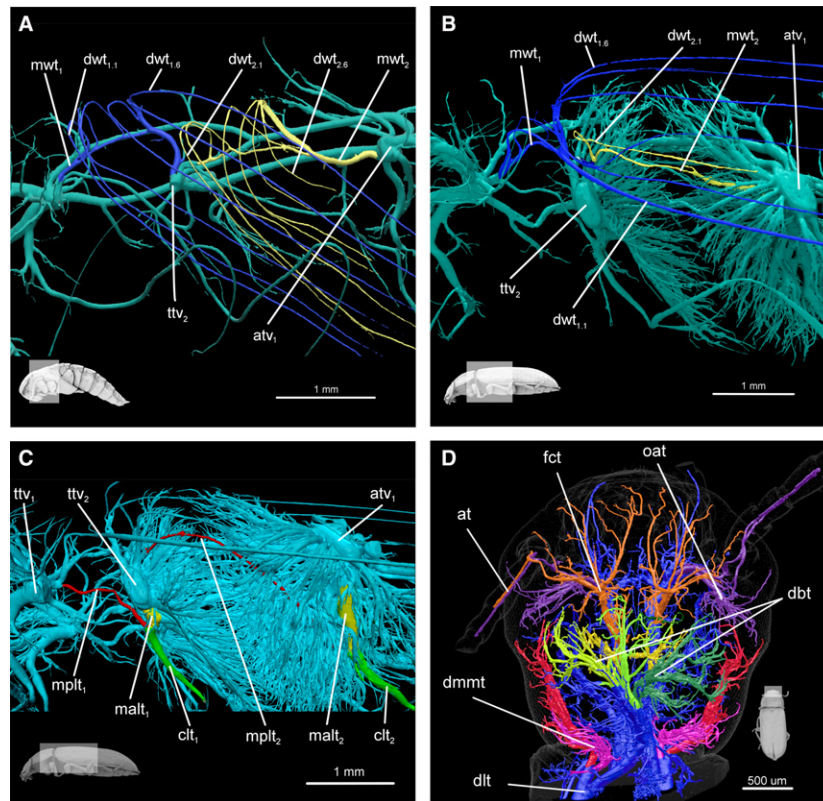


Fig. 2 Tracheae of pterothorax and head. (A) Meso- and metathorax of pupa, lateral view: fore wing trachea (blue); hind wing trachea (yellow). (B) Meso- and metathorax of imago, lateral view: fore wing trachea (blue); hind wing trachea (yellow). (C) Meso- and metathorax of imago, lateral view: anterior part of main leg trachea (yellow), posterior part of main leg trachea (red) and common leg trachea (green). (D) Teratology of head tracheae (right side) in adult. On right side, trachea heading to antenna are composed of two branches both originating from optico-antennal tracheae (purple); in other specimens (and left side) these tracheae are composed of branches originating from fronto-clypeal (orange) and optico-antennal tracheae (purple). at, antennal trachea; atv1, tracheal vestibule of one abdominal segment; clt1, mesoleg common leg trachea; clt2, metaleg common leg trachea; dbt, dorsal brain trachea; dlt, dorsal longitudinal trunk; dmmt, dorsal mandibular muscle trachea; dwt1.1, 1 distal trachea of fore wing; dwt1.6, 6 distal trachea of fore wing; dwt2.1, 1 distal trachea of hind wing; fct, fronto-clypeal trachea; malt1, main anterior mesoleg trachea; malt2, main anterior metaleg trachea; mplt1, main posterior mesoleg trachea; mplt2, main posterior metaleg trachea; mwt1, main fore wing trachea; mwt2 – main hind wing trachea; oat, optico, antennal tracheal; ttv2, metathorax tracheal vestibule.

for which non-professional terms existed. Therefore, several new names are introduced here. The newly proposed nomenclature was formed taking into consideration the relative location of a given respiratory structure with other key elements of the body, i.e. tagma (head, thorax, and abdomen), body axis (anteroposterior, dorso-ventral and left-right), appendages (e.g. antennae, maxillae, legs and wings) and internal organs (e.g. central nervous system, muscles). A comparison of the terminology used in this publication with that in other works concerning the tracheal system of insects is presented Table 3.

Common features

Tenebrio molitor is equipped in every developmental stage with 10 pairs of spiracles (holopneustic arrangement). The first two of them are distributed on the thorax (ts_1 – mesothorax; ts_2 – metathorax) and the remaining eight on the abdomen (as_1 – as_8 – located respectively on the first eight abdominal segments). Directly behind the

occluding apparatus of each spiracle, a tracheal vestibule is located. This is a spherical three-dimensional structure that gives rise to multiple tracheae which penetrate the insect's body.

Neighbouring spiracles of the subsequent body segments are connected by the dorsal (*dlt*) and ventral (*vt*) longitudinal tracheae/trunks (Figs 5 and 6). Moreover, in the case of ts_1 – ts_2 and ts_2 – as_1 , the existence of an additional longitudinal connection was discovered. This linkage is composed of the main wing trachea – dorso-lateral path (*mwt*₁, *mwt*₂) and the main leg trachea (*mlt*₁, *mlt*₂).

Spiracles of a single segment are transversely connected *via* dorsal (*dc*) and ventral (*vc*) commissures (Figs 5B,D and 6B,C). The *dc* originate directly from particular tracheal vestibules and the *vc* arise from the ventral longitudinal tracheal trunks (Figs 5B and 6B,C). In earlier larval instars some of the dorsal commissures do not seem to be fully developed. A different arrangement is observed in the prothorax and the head. The prothorax lacks the dorsal commissure

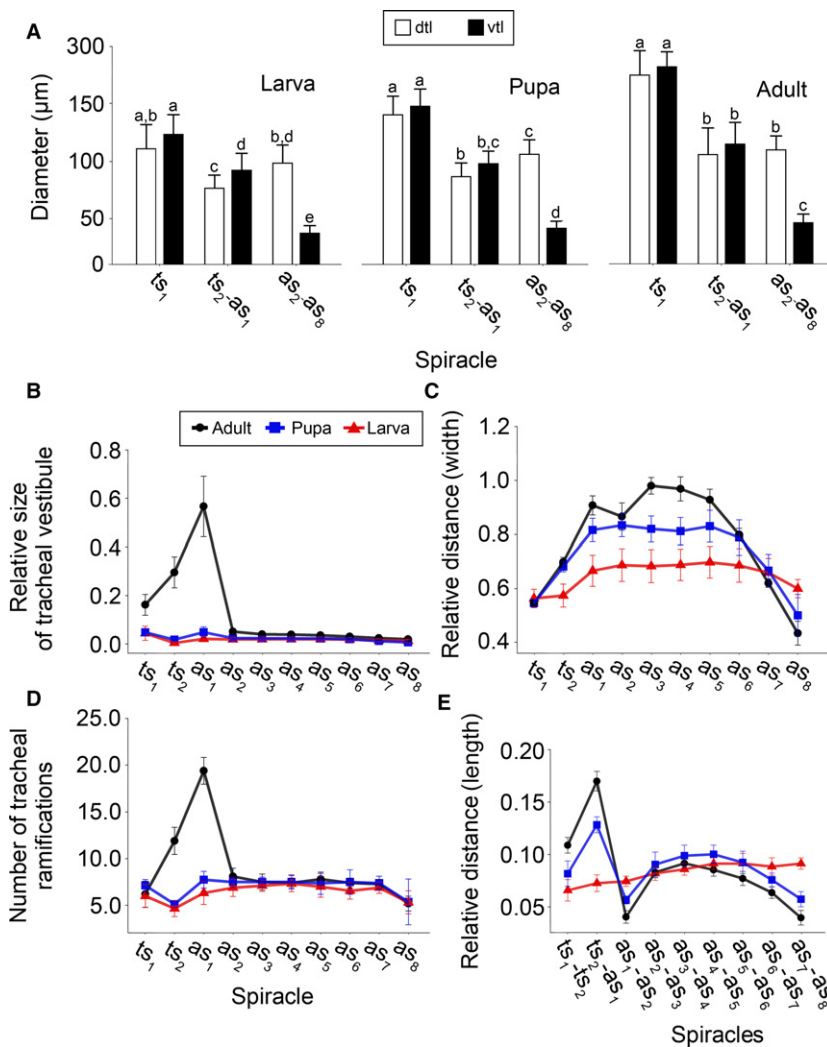


Fig. 3 Quantitative changes of the tracheal system during metamorphosis. (A) Differences in diameter of major longitudinal tracheae across different type of modules and developmental stages. Data are mean \pm SD. Measurements were taken directly at the midpoint between neighbouring spiracles, except tracheae heading anteriorly from ts₁, where diameter was measured just before the entrance of dorsal and ventral longitudinal trunks to head. Different letters indicate significant differences across particular stadium (Tukey's HSD test, $P < 0.05$). (B) Modifications of spiracles and tracheal vestibules. Relative size of tracheal vestibules presented as the ratio between volume of given tracheal vestibule and total body volume. (C) Relative distance of spiracles of same body segment presented as the ratio between distance between given pair of spiracles divided by maximum width head capsule. (D) Number of tracheal ramifications corresponds to number of tracheae originating directly in given tracheal vestibule. (E) Relative distance along longitudinal body axis (length) between spiracles corresponds to ratio of distance between neighbouring spiracles and total body length. Data are mean \pm SD. as₁–as₈, abdominal spiracles 1–8; ts₁, mesothoracic spiracle; ts₂, metathoracic spiracle; dlt, dorsal longitudinal trunk; vlt, ventral longitudinal trunk.

(dc), and in the head two following commissures were identified – the ventral head commissure (vhc) and the brain commissure (bc). Moreover, the first thoracic spiracle pair (ts₁) is additionally connected by the proleg trachea commissure (lc) (Fig. 7E).

Visceral trachea, both dorsal (dvt) and ventral (vvt), are directed anteriorly (Figs 6C and 7B). These tracheae are present in the abdomen, from the second to the last abdominal spiracle (as₂–as₈). On the other hand, the first thoracic (ts₁) and the first abdominal spiracle (as₁) are only equipped with a single trachea and the second thoracic spiracle (ts₂) has none. In all developmental stages most visceral tracheae (dorsal – dvt and ventral – vvt) were directed anteriorly.

The above-mentioned features of the tracheal system seem to be invariable across all studied developmental stages, therefore any deviations from this bauplan are interpreted here as teratologies. All the observed anomalies in this part of the tracheal system are described below.

Tracheal modules

A comparative analysis of the anatomy of the tracheal system enabled designation of a concept of a tracheal module, which is a fundamental part of the respiratory system composed of a spiracle, tracheal vestibule, and the complex of tracheae which arise from it (Fig. 6C). Although 20 different tracheal modules (10 pairs) are present in the body of *T. molitor* (Fig. 1A), they can be grouped into three major types on the basis of their unique structure, functionality and development (Figs 4 and 8), which correspond to the general division of the tracheal system.

A *cephalo-prothoracic* type of module develops exclusively around the first thoracic spiracles (ts₁) and shows the highest number of modifications. The spiracles and vestibules composing this module are located in a part of the mesothorax which is displaced anteriorly to the prothorax – the spiracles lie directly under the pronotum, behind the coxal cavity of the prolegs. Dorsal (dlt) and ventral (vlt) longitudinal tracheae, which are directed towards the body front, aerate the prothorax and the head. These tracheal

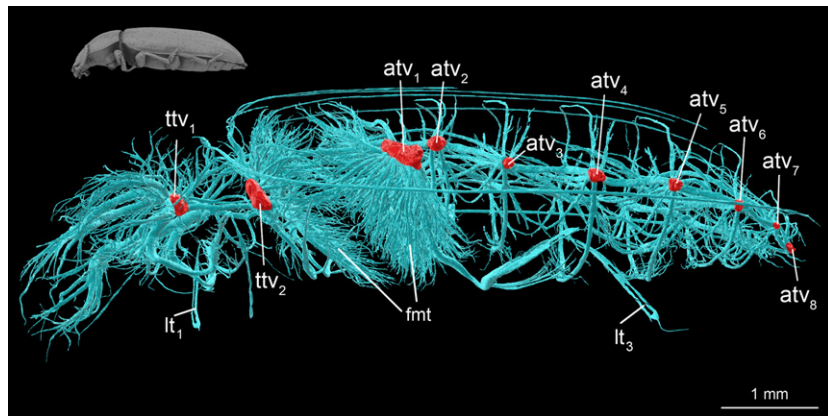


Fig. 4 Structure and location of tracheal vestibules in tracheal system of adult *Tenebrio molitor*. atv1–atv8, abdominal tracheal vestibule 1–8; fnt, flight muscles trachea; lt1, proleg trachea; lt3, metaleg trachea; ttv1, mesothorax tracheal vestibule; ttv2, metathorax tracheal vestibule.

Table 2 Mean fractal dimension value, tracheal system and body volume (\pm SD) calculated for studied developmental stages of *Tenebrio molitor*.

Stadium	Tracheal system fractal dimension	Tracheal system volume (mm ³)	Body volume (mm ³)
Larva, df = 9	2.02 ^A \pm 0.08	1.08 ^A \pm 0.50	173.19 \pm 70.04
Pupa, df = 8	2.10 ^A \pm 0.04	1.41 ^A \pm 0.32	171.01 \pm 44.98
Adult, df = 9	2.20 ^B \pm 0.3	3.39 ^B \pm 0.78	122.99 \pm 23.31

Different letters indicate significant differences (Tukey's HSD test, $P < 0.05$).

trunks were noticed to have greater diameters than their homologues identified in other modules (Fig. 3A). This tendency was observed in all developmental stages; however, in the case of larvae these differences were not statistically significant (Tukey HSD test, $P > 0.05$).

In the prothorax, the ventral longitudinal trunks (*vlt*) are connected by a ventral commissure (*vc*) and an additional connection (leg commissure – *lc*) that is present between the fore leg tracheae (*lt*) near their proximal end (Fig. 7E). In the head, ventral longitudinal tracheae are connected in the anterior ends by the ventral head commissure (*vhc*). In the dorsal part of the head, two dorsal brain tracheae (*dbt*) are connected by the brain commissure (*bc*) (Figs 2D and 6A). A dorsal commissure (*dc*) is absent.

The dorsal longitudinal trachea (*dlt*) prior to reaching the occipital foramen divides into two tracheae (Figs 2D, 6A and 7E), the first heading to the brain (dorsal brain trachea, *dbt*) and the second one to mandibular muscles (dorsal mandibular muscle trachea, *dmmt*). The dorsal brain trachea is located medially in the dorsal part of the head, originating just before the occipital foramen. It subsequently sprouts into many smaller tracheae which form a flat delta-arranged cluster lying on the brain surface (Fig. 2D). From the ventral longitudinal trachea, in the vicinity of the occipital foramen, three tracheae sprout, heading laterally to the mandibular muscles: anterior (*avmt*), medial (*mvmt*) and

posterior mandibular muscle trachea (*pvmt*). At the level of the brain, from *vht* the ventral brain trachea (*vbt*) sprouts outwards (Figs 2D and 6A). This trunk is directed dorsally. It is a relatively long and straight trachea, which divides into many smaller ones when it reaches the ventral surface of the brain. Another trachea which originates from the *vlt* is named herein as the fronto-clypeal trachea (*fct*). It is heading antero-dorsally to reach the surface of the head capsule. Within the dorsal part of the head it divides into numerous tracheae that are distributed beneath the frons and clypeus, and also penetrate the labrum. Additionally, one of these branches heads towards the antenna. In its distal end, the *vlt* is divided into tracheae that are aerating mouthparts, i.e. labium trachea (*lat*), maxillary trachea (*mat*) and mandibular trachea (*mnt*). Moreover, the opto-antennal trachea (*oat*) derives from this part of the *vlt*. This trunk has branches to the compound eye and antenna (the second trachea). The suboesophageal ganglion is aerated by a few tracheae which sprout from the ventral commissure (in the prothorax) and head anteriorly between ventral longitudinal tracheae.

The fore legs are penetrated by the proleg trachea (*lt*₁), which derives from the ventral longitudinal trachea (Figs 4, 5A and 8). The tracheae aerating muscles, which are responsible for leg movement (e.g. extrinsic leg muscles *m. pleurotrochanteralis*, *m. noto-coxalis*, *m. episterno-coxalis*), originate from the *vlt* and its direct ramifications. The front part of these muscles is penetrated by two tracheae – the first one diverges directly from the *vlt* (anterior prothorax muscle trachea *vlt-apmt*₁), whereas the second one (anterior prothorax muscle trachea *lt*₁-*apmt*₂) diverges from the leg trachea (*lt*₁). Both these trunks are primarily headed anteriorly, changing direction in their distal parts to head latero-dorsally.

The dorsal longitudinal trachea (*dlt*) gives rise to numerous (~ 10) trunks that penetrate the muscles of the prothorax. These tracheae originate from *dlt* along the entire length of prothorax. Additionally, the three largest branches which aerate these muscles arise directly from the latero-posterior wall of the first tracheal vestibule (*ttv*₁) –

Table 3 List of abbreviations and morphological terms used in this publication compared with terms used in other works concerning the tracheal system of insects.

Abbreviation	Full name	References/Alternative term
<i>adc</i>	Abdominal dorsal commissure	Newly introduced
<i>adlt</i>	Abdominal dorsal longitudinal trunk	Alternative term: large lateral longitudinal trunks (Tonapi, 1977)
<i>apmt₁</i>	Anterior prothorax muscle trachea from <i>vt</i>	Newly introduced
<i>apmt₂</i>	Anterior prothorax muscle trachea from leg	Newly introduced
<i>as₁–as₈</i>	First–eighth abdominal segment spiracle	Snodgrass (1935)
<i>at</i>	Antennal trachea	Newly introduced
<i>atv₁–atv₈</i>	First–eighth abdominal segment tracheal vestibule	Newly introduced
<i>avc</i>	Abdominal ventral commissure	Newly introduced
<i>avlt</i>	Abdominal ventral longitudinal trunc	Newly introduced
<i>avmt</i>	Anterior ventral mandibular muscle trachea	Newly introduced
<i>bc</i>	Brain commissure	Alternative terms: dorsal head commissure (Hafeez & Gardiner, 1964), dorsal cervical anastomosis (Whitten, 1968)
<i>clt</i>	Common leg trachea	Lateral leg trachea (Snodgrass, 1935)
<i>cwlt</i>	Common leg-wing trachea	Newly introduced
<i>dat</i>	Dorso-anterior trachea	Newly introduced
<i>dbt</i>	Dorsal brain trachea	Newly introduced
<i>dc</i>	Dorsal commissure	Alternative term: dorsal anastomosis (Whitten, 1968), dorsal tracheal commissure (Snodgrass, 1935)
<i>dht</i>	Dorsal head trachea	Alternative term: dorsal cephalic trachea (Tonapi, 1977), dorsal cervical (Whitten, 1968)
<i>dlt</i>	Dorsal longitudinal trunk	Whitten (1968) Alternative terms: lateral longitudinal trachea (Loudon, 1989), dorsal lateral trunk/lateral trunk (Hafeez & Gardiner, 1964), large lateral longitudinal trunks (Tonapi, 1977), dorsal longitudinal trachea (Chapman, 1918), lateral plurisegmental tracheal trunk (Snodgrass, 1935)
<i>dlt_a</i>	Dorsal longitudinal trunk anterior part	Newly introduced
<i>dlt_p</i>	Dorsal longitudinal trunk posterior part	Newly introduced
<i>dmmt</i>	Dorsal mandibular muscle trachea	Newly introduced
<i>dpmt</i>	Dorsal prothorax muscle trachea	Newly introduced
<i>dpt</i>	Dorso posterior trachea	Newly introduced
<i>dvt</i>	Dorsal visceral trachea	Tonapi (1977) Alternative term: visceral trachea (Hafeez & Gardiner, 1964; Loudon, 1989)
<i>dwt</i>	Distal wing trachea	Newly introduced
<i>fct</i>	Fronto-clypeal trachea	Newly introduced
<i>fmt</i>	Flight muscles trachea	Newly introduced
<i>lat</i>	Labial trachea	Newly introduced
<i>lc</i>	Proleg commissure	Newly introduced
<i>lpmt</i>	Lateral prothorax muscle trachea	Newly introduced
<i>lt</i>	Legs trachea	Whitten (1968)
<i>lt₁</i>	Proleg trachea	Chapman (1918)
<i>lt₂</i>	Mesoleg trachea	Chapman (1918)
<i>lt₃</i>	Metaleg trachea	Chapman (1918)
<i>malt</i>	Main proleg trachea	Basal wing trachea (Snodgrass, 1935)
<i>malt₁</i>	Main anterior mesoleg trachea	Newly introduced
<i>malt₂</i>	Main anterior metaleg trachea	Newly introduced
<i>mat</i>	Maxillary trachea	Newly introduced
<i>mlt</i>	Main leg trachea	Newly introduced
<i>mlt₁</i>	Main mesoleg trachea	Newly introduced
<i>mlt₂</i>	Main metaleg trachea	Newly introduced
<i>mnt</i>	Mandibular trachea	Newly introduced
<i>mplt</i>	Main posterior leg trachea	Newly introduced
<i>mplt₁</i>	Main posterior mesoleg trachea	Newly introduced
<i>mplt₂</i>	Main posterior metaleg trachea	Newly introduced

(continued)

Table 3 (continued)

Abbreviation	Full name	References/Alternative term
<i>mvmt</i>	Median ventral mandibular muscle trachea	Newly introduced
<i>mwt</i>	Main wing trachea	Alternative term: transverse basal trachea + costo-radial + cubito-anal (Chapman, 1918)
<i>mwt₁</i>	Main fore wing trachea	Newly introduced
<i>mwt₂</i>	Main hind wing trachea	Newly introduced
<i>mawt</i>	Main anterior wing trachea	Alternative term: costo radial trachea (Chapman, 1918)
<i>mpwt</i>	Main posterior wing trachea	Alternative term: cubito-anal trachea (Chapman, 1918)
<i>oat</i>	Optico-antennal trachea	Newly introduced
<i>pvmt</i>	Posterior ventral mandibular muscle trachea	Newly introduced
<i>rlt</i>	Rudimentary leg trachea	Newly introduced
<i>rwt</i>	Rudimentary wing trachea	Newly introduced
<i>sp</i>	Spiracle	Snodgrass (1935)
<i>stg</i>	Suboesophageal ganglion trachea	Newly introduced
<i>tdc</i>	Thoracic dorsal commissure	Newly introduced
<i>ts₁</i>	Mesothorax spiracle	Snodgrass (1935) and Hafeez & Gardiner (1964)
<i>ts₂</i>	Metathorax spiracle	Snodgrass (1935) and Hafeez & Gardiner (1964)
<i>ttv₁</i>	Mesothorax tracheal vestibule	Newly introduced
<i>ttv₂</i>	Metathorax tracheal vestibule	Newly introduced
<i>tv</i>	Tracheal vestibule	Alternative term: spiracular trachea (Hafeez & Gardiner, 1964; Tonapi, 1977)
<i>vbt</i>	Ventral brain trachea	Newly introduced
<i>vc</i>	Ventral commissure	Hafeez & Gardiner (1964) and Tonapi, (1977) Alternative term: ventral tracheal anastomosis/ventral ganglionic (Whitten, 1968), ventral tracheal commissure (Snodgrass, 1935)
<i>vhc</i>	Ventral head commissure	Hafeez & Gardiner (1964)
<i>vht</i>	Ventral head trachea	Alternative terms: ventral cephalic trachea (Tonapi, 1977), ventral cervical (Whitten, 1968)
<i>vlt</i>	Ventral longitudinal trunk	Alternative terms: ventral lateral trunk (Hafeez & Gardiner, 1964), lateral longitudinal trunk (Whitten, 1968), ventral longitudinal trachea (Chapman, 1918), ventral plurisegmental tracheal trunk (Snodgrass, 1935)
<i>vlt_a</i>	Ventral longitudinal trunk anterior part	Newly introduced
<i>vlt_p</i>	Ventral longitudinal trunk posterior part	Newly introduced
<i>vpmt</i>	Ventral prothorax muscle trachea	Newly introduced
<i>vvt</i>	Ventral visceral trachea	Alternative terms: visceral trachea (Snodgrass, 1935; Hafeez & Gardiner, 1964; Loudon, 1989)
<i>wt</i>	Wing trachea	Whitten (1968) and Tonapi (1977)

the ventral prothorax muscle trachea (*vpmt*) heading ventralo-posteriorly then sprouting a trachea headed anteriorly, which aerates the posterior and latero-ventral part of prothorax; the lateral prothorax muscle trachea (*lpmt*) located laterally and sprouting a trachea in an anterior direction; the dorsal prothorax muscle trachea (*dpmt*) directed dorsally at the proximal end and then heading anteriorly, aerating the lateral part of the prothorax muscles.

Metathoracic type is characterised as follows. All tracheae which branch from the metathoracic (*ttv₂*) and the first abdominal (*as₁*) segment tracheal vestibules construct a coherent and consistent system, which is connected to the flight apparatus and meso- and metalegs. This part of the tracheal system is composed of a unique type of tracheal module (Figs 2A–C and 6B).

Dorsal and ventral longitudinal tracheae have a specific topology around the *ttv₂*. Prior to connecting with a tracheal vestibule, each pair of dorsal (*dlt_a*–*dlt_p*) and ventral (*vlt_a*–*vlt_p*) trunks merges into a single trachea. In conclusion, the metathoracic vestibule is connected to only two tracheal trunks (dorsal and ventral), not four (*dlt_a*, *dlt_p*, *vlt_a*, *vlt_p*) as in other tracheal vestibules (Fig. 5A,C).

Respiratory gases are transported into the middle leg pair via tracheae which arise in meso- (*ts₁*) and metathorax (*ts₂*), whereas metalegs are aerated by trunks originating in metathorax (*ts₂*) and the first abdominal segment (*as₁*) (Figs 2C, 5A and 6B). Specifically, a particular tracheal vestibule gives rise to the anterior (*mlt_a*) and posterior part of the main leg trachea (*mlt_p*), which then connects, forming the main leg trachea (*mlt*) (Figs 2C and 6B). In larval forms,

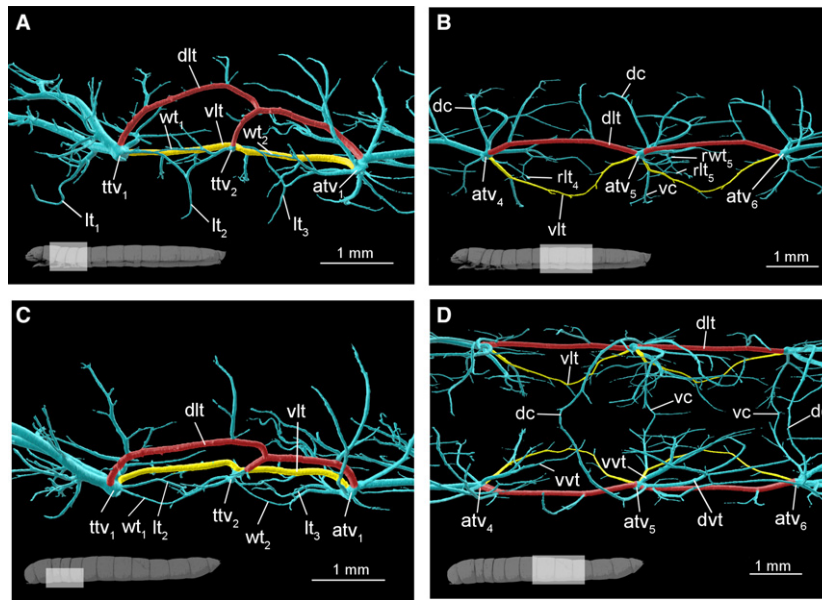


Fig. 5 Anatomy of larval tracheal system. (A,C) Meso- and metathorax (A) lateral and (C) dorsal views. (B, D) Abdomen, segments 4–5, (B) lateral and (D) dorsal views: dorsal (red) and ventral (yellow) longitudinal tracheal trunks. atv1, tracheal vestibule of first abdominal segment; atv4–atv6, abdominal tracheal vestibule 4–6; dc, dorsal commissure; dlt, dorsal longitudinal trunk; dvt – dorsal visceral trachea; lt1, proleg trachea; lt2, meso-leg trachea; lt3, metaleg trachea; rlt4–rlt5, rudimentary leg trachea in 4–5 abdominal segment; rwt5, rudimentary wing trachea in 5 abdominal segment; ttv1, mesothorax tracheal vestibule; ttv2, metathorax tracheal vestibule; vc, ventral commissure; vlt, ventral longitudinal trunc; vvt, ventral visceral trachea wt1, fore wing trachea; wt2, hind wing trachea.

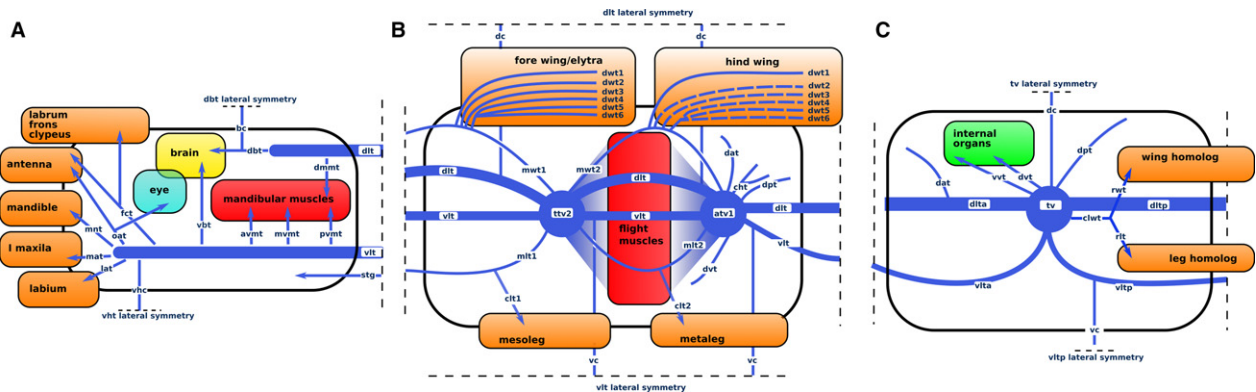


Fig. 6 Schematic organisation of different types of tracheal modules. (A) Cephalo-prothoracic, (B) thoracic and (C) abdominal module. Dotted lines in the case of hind wing present trachea which undergo loss in pupa–imago transition. avmt, anterior ventral mandibular muscle trachea; bc, brain commissure; cwlt, common leg-wing trachea; clt1, common mesoleg trachea; clt2, common metaleg trachea; dat, dorso anterior trachea; dbt, dorsal brain trachea; dc, dorsal commissure; dlt, anterior part of dorsal longitudinal trunk; dltp, posterior part of dorsal longitudinal trunk; dmmt, dorsal mandibular muscle trachea; dpt, dorso posterior trachea; dvt, dorsal visceral trachea; dwt1–6, distal wing trachea 1–6; fct, fronto-clypeal trachea; lat, labial trachea; mat, maxillary trachea; mlt1, main anterior mesoleg trachea; mlt2, main anterior metaleg trachea; mnt, mandibular trachea; mvmt, median ventral mandibular muscle trachea; mwt1, main fore wing trachea; mwt2, main hind wing trachea; oat, optico, antennal ganglion trachea; pvmt, posterior ventral mandibular muscle trachea; rlt, rudimentary leg trachea; rwt, rudimentary wing trachea; stg, suboesophageal ganglion trachea; tv, tracheal vestibule; vbt, ventral brain trachea; vc, ventral commissure; vlt, anterior part of ventral longitudinal trunk; vlt, posterior part of ventral longitudinal trunk; vvt, ventral visceral trachea.

these tracheae have similar diameters and lengths (Fig. 2C), whereas in adults they differ from one another (Fig. 7B). In meso- and metaleg *malts* are much wider and shorter than *mplts*. In summary, the middle pair of legs is mostly aerated by *mal*₁ from the *ttv*₂ and the metaleg by *mal*₂ from *atv*₁ (Fig. 7B).

A comparative study of different stages of development in *T. molitor* revealed that the tracheae responsible for wing aeration are also present in larvae (Figs 5A,C and 7B). These trunks are composed mainly of the main wing trachea (fore wing, *mwt*₁ and hind wing, *mwt*₂) with three to four short distal ramifications (*dwt*). The main wing

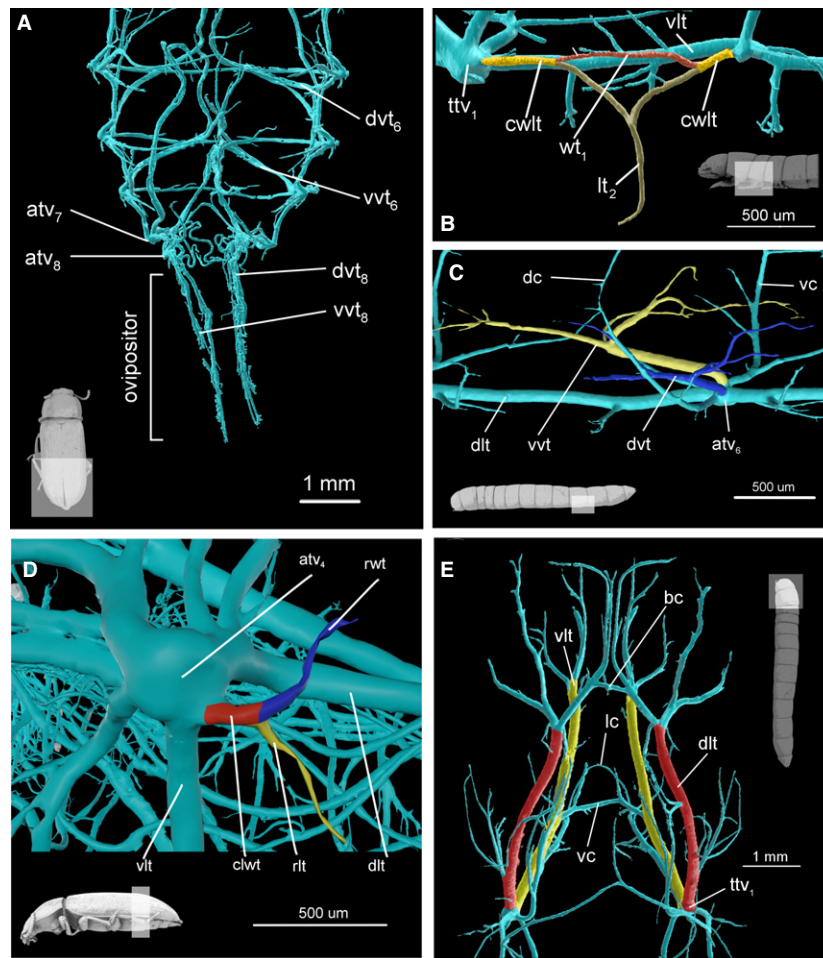


Fig. 7 Anatomy of tracheal system. (A) Abdomen of imago, dorsal view. Specimen has extruded ovipositor and aerating trachea are pulled with it. (B) Mesothorax of larva lateral view. In colour, mesoleg (brown) and fore wing trachea (red) and common wing leg trachea (yellow). (C) Abdomen of larva, segment 5, dorsal view. In colour, dorsal visceral trachea (blue) and ventral visceral trachea (blue). (D) Tracheal vestibule of abdominal segment 4 of imago, lateral view. In colour, leg homologues trachea (yellow), wing homologues trachea (blue) and common wing leg homologue trachea (red). (E) Head and prothorax of larva, dorsal view. In color, longitudinal tracheal trunks, dorsal (red) and ventral (yellow). atv4, tracheal vestibule of 4 abdominal segment; atv6–atv8, tracheal vestibule of 6–8 abdominal segment; bc, brain commissure; lwt, common leg-wing trachea; cwlt, common leg-wing trachea; dc, dorsal commissure; dlt, dorsal longitudinal trunk; dvt, dorsal visceral trachea; dvt6 and dvt8 – dorsal visceral trachea of 6 and 8 abdominal segment; lc, proleg commissure; lt1, proleg trachea; rit, rudimentary leg trachea; rwt, rudimentary wing trachea; ttv1, tracheal vestibule of mesothorax; vc, ventral commissure; vlt, ventral longitudinal trunk; vvt, ventral visceral trachea; vvt6 and vvt8 – ventral visceral trachea of 6 and 8 abdominal segment; wt1, fore wing trachea.

tracheae in larvae prior to connecting to the tracheal vestibule merge with the main leg tracheae (mwt_1 – mlt_1 , mwt_2 – mwt_2). In pupae and adults, wing and leg tracheae connect to tracheal vestibules separately (Fig. 2A–C). In pupae, each wing is penetrated by six distal wing tracheae (dwt), whereas in larvae by only three or four (Fig. 2A). Conversely, in adults these trunks were reduced to a single one, which runs parallel to the subcostal vein (Fig. 2B). The number of trachea penetrating the adult fore wing is the same as in the pupa ($dwt_{1.1}$ – $dwt_{1.6}$). Three distal wing trachea ($dwt_{1.4}$, $dwt_{1.5}$, $dwt_{1.6}$) that lie medially in the wing, diverge from the main wing trachea (mwt_1) as a one branch. The same topology can be seen in hind wing for distal trachea ($dwt_{2.4}$, $dwt_{2.5}$, $dwt_{2.6}$). The respiratory system of each wing

is connected to two tracheal vestibules i.e., fore wing with ttv_1 and ttv_2 and hind wing with ttv_2 and atv_1 (Fig. 2A,B).

Abdominal type. The tracheal module originates on spiracles occurring on the abdominal segments from the second to the eighth (as_2 – as_8) (Figs 1A and 8) and is opposed to the following tracheae: the dorsal longitudinal trunk (dlt) (anterior dlt_a and posterior dlt_p part), the ventral longitudinal trunk (vlt) (anterior vlt_a and posterior vlt_p part), dorsal commissure (dc), the dorsal (dvt) and ventral visceral trachea (vvt), the common leg-wing trachea, or the common leg-wing trachea (cht or $cwlt$) and the dorso-posterior trachea (dpt). Moreover, the ventral commissure (vc) derives from the ventral longitudinal trunk just after the tracheal vestibule. Similar topology has been observed

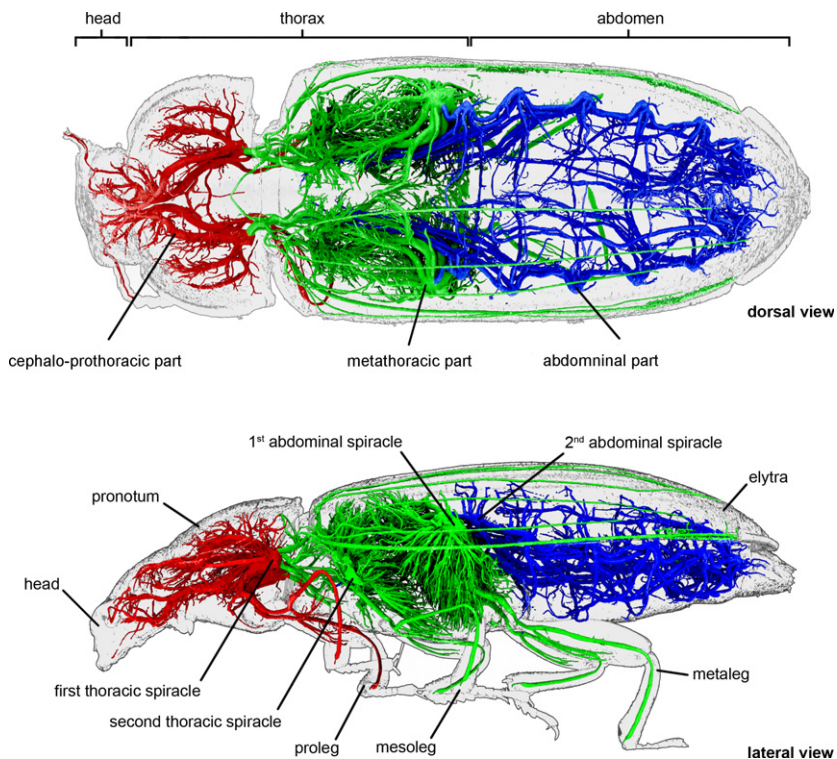


Fig. 8 Tracheal system of adult *Tenebrio molitor*. In colour, parts of tracheal system characterized by different type of tracheal modules (cephalo-prothoracic – red, thoracic – green, abdominal – blue).

in the case of the dorso-anterior trachea (*dat*), which derives from the dorsal longitudinal anterior trunk (*dlt*) (Figs 6C and 5B,D).

All developmental stages were observed to possess Y-shaped tracheae (*cwlt* which subsequently divide into *rlt* and *rwt*) that arise from the posterior wall of particular tracheal vestibules (Figs 6C and 7D). These trunks are structured in the same manner as the common leg-wing tracheae (*cwlt*, *lt*, *wt*) of the modules of the metathoracic and the first abdominal spiracles (Fig. 7B). *Ch*t are most noticeable in the pupal stage when they aerate the denticular outgrowths of the abdomen.

In adults, visceral tracheae originating from *atv*₂–*atv*₅ extend beyond mesothorax and aerate the digestive system. On the other hand, the visceral trunks of *atv*₈ connects with the terminalia and can be projected with them (Fig. 7A).

As far as the diameter is concerned, ventral longitudinal tracheal (*vlt*) trunks occurring in abdominal segments from the first to the eighth have the smallest diameter compared with their homologues in the other body segments (Tukey HSD, $P > 0.05$; Fig. 3A).

Teratologies

In the case of a single larval specimen, a few additional longitudinal connections between tracheal vestibules *atv*₁–*atv*₂, *atv*₂–*atv*₃ and *atv*₅–*atv*₆ were identified. Those teratologies are restricted to one side of the body, whereas the other half remains unchanged. In all of the above-

mentioned spiracle pairs, the additional linkage is made up of the fusion of dorsal-posterior tracheae and dorsal commissures (Fig. 9A). Longitudinal tracheal connections of the same nature were also reported between tracheal vestibule pairs *atv*₁–*atv*₂ and *atv*₂–*atv*₃ of a single pupa (Fig. 9B). Similarly to the larval specimen, only one side of the body was affected. Moreover, concerning the same pupa specimen, the tracheal system of the hind leg is unusually made up of an outgrowth of the *ttv*₂–*atv*₁ ventral longitudinal trunk. The main leg trachea (*mlt*₂) trachea is present; however, the common leg trachea (*clt*₂) does not originate from it (Fig. 9B). On the contrary, the trachea that penetrates the leg arises from the ventral longitudinal tracheal trunk (*vlt*). This teratology was identified on the same body side as the previous one.

Teratological modification of the antennal trachea was reported in the case of a single adult. In this individual, the right antenna is aerated by a pair of tracheae sprouting from a single basal trunk (optico-antennal trachea, *oat*). In all the other investigated specimens (larvae, pupae and imago) antennae are supported by two separate tracheae originating respectively from fronto-clypeal (*fct*) and optico-antennal tracheae (*oat*) (Fig. 2D).

As was mentioned before, the development of higher order branches (including tracheoles) is mostly influenced by non-genetic factors (e.g. hypoxia). This part of the tracheal system was extremely variable across the individuals analysed and therefore its structural variability is not described at present.

Development

Spiracles distribution

Distances between the spiracles change significantly through metamorphosis (longitudinally, $F = 70.67$, $df = 2$, $P < 0.001$; transversally, $F = 24.8$, $df = 2$, $P < 0.001$) (Fig. 3C, E). The investigation of the relative distance between spiracles of the neighbouring body segments revealed a more complex image. ANOVA showed a significant effect of stadium ($F = 4.55$, $df = 2$, $P < 0.05$) and spiracle ($F = 168.98$, $df = 8$, $P < 0.001$). In larvae, the distances of subsequent spiracles slightly increase, reaching the maximum value in the last abdominal pair (Fig. 3E). The images acquired for pupae and adults are similar (Fig. 3E). Both of them show statistically significant higher values for ts_1 – ts_2 and ts_2 – as_7 ($P < 0.05$), and lower values for as_7 – as_8 ($P < 0.05$) compared with larvae. The *post hoc* pairwise comparison revealed that the distances reported for pupae and adults differ significantly in each investigated pair of spiracles ($P < 0.05$).

Relative distances between spiracles in the transverse plane (distance of spiracles from the same segment to the head capsule width) varied between studied developmental stages (ANOVA, $F = 180.55$, $df = 2$, $P < 0.001$) and pairs of spiracles (ANOVA, $F = 191.78$, $df = 9$, $P < 0.001$). When comparing the relative width between the spiracles of the same body segment, it was noted that the distance within ts_2 – as_6 pairs greatly increases (Fig. 3E). However, *post hoc* pairwise comparison did not reveal significant differences among ts_2 and as_6 in pupae and adults ($P > 0.05$). The relative width reported between the spiracles of the first thoracic and seventh abdominal pair are relatively constant across all studied developmental stages (Tukey HSD, $P > 0.05$) (Fig. 3E). On the other hand, the relative width between the eight abdominal spiracles of the opposite body sides decreases during metamorphosis ($P < 0.05$). In adults, as_8 are directly responsible for supplying terminalia with respiratory gases.

Tracheal vestibule volume and connections

While comparing the relative size of tracheal vestibules within developmental stages, significant differences were identified (ANOVA, $F = 334.56$, $df = 2$, $P < 0.01$). It was noted that the volume of the first three pairs (ts_1 , ts_2 , as_1) strongly increases after the pupal stadium. The highest value of vestibule to the body volume ratio was reported for as_1 , then ts_2 and finally ts_1 (Fig. 3B). *Post hoc* pairwise comparison revealed significant differences among these vestibules ($P < 0.001$). In adults ts_2 (atv_2) and as_1 (atv_2) are directly responsible for supporting the flight muscles with respiratory gases (Figs 2B,C, 4 and 10). The tracheal vestibules of larva, pupa and these in adults' abdomens are homogeneous (Fig. 3B) and showed no differences when analysed with Tukey HSD ($P > 0.05$).

The investigation of the number of tracheal ramifications originating in a particular vestibule revealed similar

dynamics. Significant differences were reported between the studied developmental stages ($F = 28.33$, $df = 2$, $P < 0.01$). The highest number of ramifications was revealed for as_1 and ts_2 in adults (Fig. 3D). *Post hoc* pairwise comparison revealed significant differences among the vestibules of these spiracles ($P < 0.001$). However, in this case ts_1 showed no differences when compared with the majority of abdominal spiracles, i.e. as_3 – as_7 ($P > 0.05$). The lowest number of ramifications was reported for the last abdominal spiracle in larvae (Fig. 3D).

Tracheal thickness distribution

An ANOVA test revealed significant differences in the mean maximal diameter of tracheae across developmental stages investigated ($F = 46.68$, $df = 2$, $P < 0.001$): larvae – $x = 0.18 \pm 0.04$ mm, pupae – $x = 0.21 \pm 0.05$ mm, adults – $x = 0.36 \pm 0.05$ mm. However, *post hoc* pairwise comparison revealed significant differences between larvae-adults and pupae-adults ($P < 0.001$), which were non-significant for larvae-pupae ($P = 0.32$).

Trachea diameter ranged between 0.025 and 0.220 mm in larva, 0.025 and 0.260 mm in pupa and 0.025 and 0.410 mm in adults. The highest count of tracheae (~ 19%) was noted for a diameter of 0.065 mm for the larval stage, whereas in pupa and imago, dominant (~ 15 and ~ 13.5%, respectively) the tracheal diameter is 0.039 mm.

The Kolmogorov–Smirnov test indicated significant differences in the trachea thickness distribution between adults and the remaining stages (Fig. 1B): pupae-adults ($D = 0.27$, $P < 0.001$), larvae-adults ($D = 0.32$, $P < 0.001$). On the other hand, disparities observed between larvae and pupae proved to be non-significant ($D = 0.15$, $P = 0.15$).

Visceral trachea

An ANOVA test showed significant differences in lengths of the visceral tracheae within different developmental stages ($F = 64.55$, $df = 2$, $P < 0.001$). The mean values of the trunks measured in larvae ($x = 2.48 \pm 0.84$ mm) and pupae ($x = 2.54 \pm 1.04$ mm) were lower than those reported for adults ($x = 3.81 \pm 1.47$ mm) (Tukey's HSD test, $P > 0.05$).

In pupae and adults the pairwise comparison showed significant differences between the mean lengths of the dorsal and ventral visceral trunks (Tukey's HSD test, $P < 0.05$). In both those cases, higher mean values were reported for the ventral trunks: pupae – dorsal tr. $x = 2.22 \pm 0.96$, ventral tr. $x = 2.97 \pm 1.01$; adults – dorsal tr. $x = 3.55 \pm 1.71$, ventral tr. $x = 4.16 \pm 1.00$. The differences reported for larvae are non-significant ($P > 0.05$): dorsal tr. $x = 2.43 \pm 0.93$, ventral tr. $x = 2.56 \pm 0.72$ (Fig. 10B).

Tracheal system volume

Even though the mean total body volume decreases in subsequent developmental stages (larva – $x = 173.19 \pm 70.04$ mm³; pupa – $x = 171.01 \pm 44.98$ mm³; adult – $x = 122.99 \pm 23.31$ mm³), the mean active volume of the

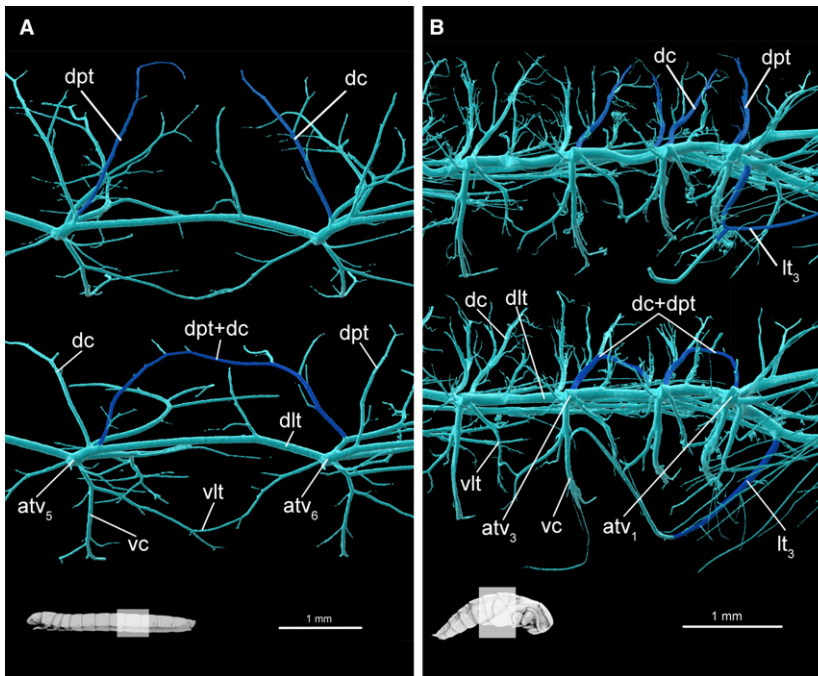


Fig. 9 Tracheal system teratologies in larva and pupa. (A) Opposite sides of larval abdominal segment 6, lateral view. Normal arrangement presented on upper image. (B) Opposite sides of pupal abdominal segments 1–3, lateral view. In colour, trachea which have different arrangements in same body segment of a single specimen. atv1–atv6, tracheal vestibule of 1–6 abdominal segment; dc, dorsal commissure; dlt, dorsal longitudinal trunk; dpt, dorso-posterior trachea; lt₃, metaleg trachea; vc, ventral commissure; vlt, ventral longitudinal trunk.

tracheal system increases throughout metamorphosis ($F = 47.66$, $df = 2$, $P < 0.001$): larva – $x = 1.08 \pm 0.50 \text{ mm}^3$, pupa – $x = 1.41 \pm 0.32 \text{ mm}^3$ and adult – $x = 3.39 \pm 0.78 \text{ mm}^3$ (Table 2).

Growth of the whole tracheal system in the case of the larva–pupa transition in relation to the body was isometric (scaling coefficient 1.16, $r = 0.18$, $df = 17$, $P > 0.05$), whereas in the pupa–imago transition, positive allometry was registered (scaling coefficient = -2.18 , $r = 0.68$, $df = 16$, $P < 0.01$) (Fig. 10A).

Fractal dimension index

Values of the fractal dimension index showed a rising trend when comparing the whole tracheal system of the subsequent developmental stages. Reported average values were as follows: larva – $x = 2.02 \pm 0.08$, pupa – $x = 2.10 \pm 0.04$, imago – $x = 2.20 \pm 0.3$ (Table 2). The fractal dimension analysis revealed significant differences in the trachea density and topology across the investigated developmental stages ($F = 27.42$, $df = 2$, $P < 0.001$). Tukey's HSD revealed significant differences between larva–imago and pupa–imago (Table 2).

Discussion

Until now, only a few studies have been made of the anatomy of the tracheal system (e.g. Szwawicz, 1956; Whitten, 1957, 1968; Hafeez & Gardiner, 1964; Srivastava, 1975; Tonapi, 1977) and its elements (e.g. Wigglesworth, 1954; London, 1989; Affolter & Shilo, 2000; Pereanu et al. 2007). For this reason, and because of methodological differences, the comparisons of the results presented above with current

knowledge of the tracheal system can only be made on a general level. It can be stated that μCT systems provide more reliable and testable data (Supplements: Raś, 2017) on the anatomy of insect respiratory systems than traditional sectioning – especially when comparing whole systems simultaneously.

The role of the haemolymphatic system in oxygen distribution in the insect body is almost negligible, unlike in vertebrates whose vascular system is the main means of delivery of respiratory gases to tissues (Pick et al. 2009). The tracheal system combines two roles – the uptake and delivery of respiratory gases – which are separated in vertebrates (to respiratory and circulatory system, Maina, 2002). This property had led to a complex anatomy of the insect respiratory system (Figs 1A and 9). The three-dimensional structure of the tracheal system reflects the demand for oxygen of specific tissues and, therefore, indirectly indicates the function and metabolic rates of certain parts of the body. As was revealed here, the brain, mandibular muscles, flight muscles and reproductive system are all connected to their own specific tracheae (Figs 2D, 4, 6A,B and 7A).

Arrangement of the tracheal system

The general scheme of the tracheal system is founded on spiracles and tracheal vestibules connected via longitudinal tracheal trunks. As the spiracles of subsequent body segments are considered serial homologues (Pitsouli & Perrimon, 2010) based on the principle of connections and similar development, the same assumption was made here concerning their major ramifications (Fig. 6). According to Wagner's (1996) conception, such structured biological

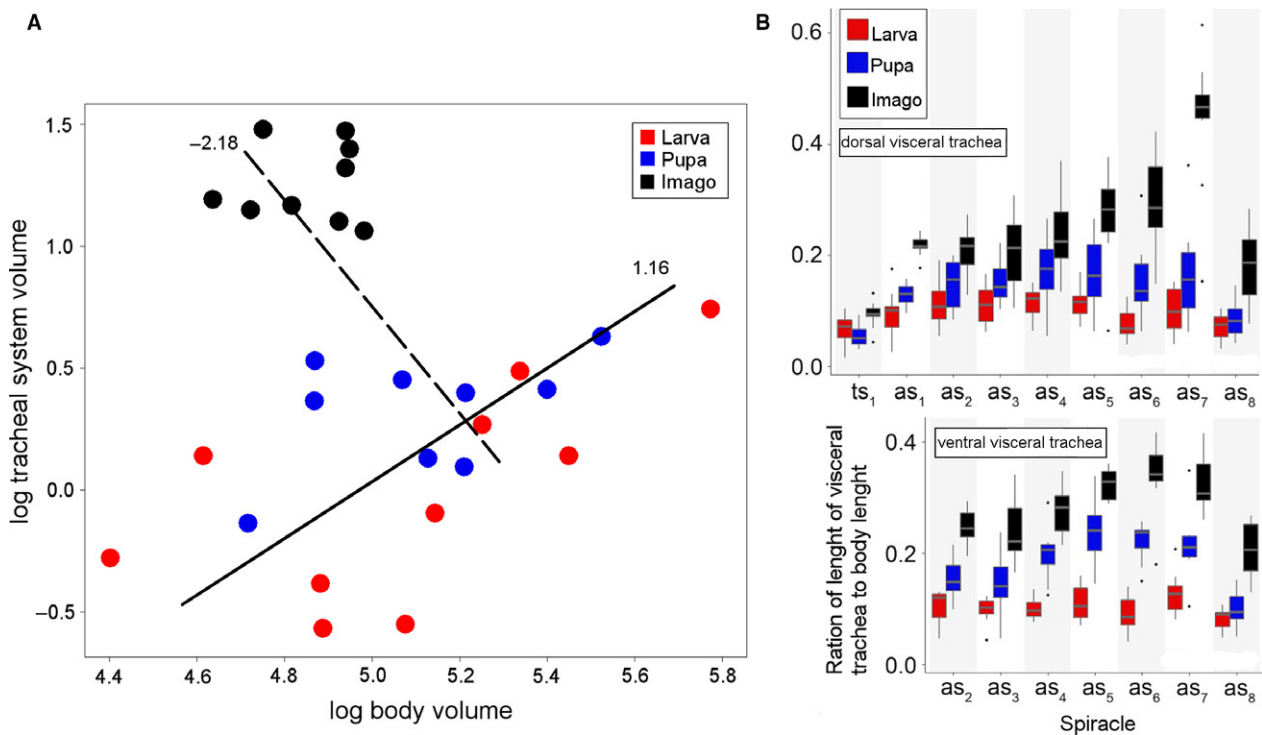


Fig. 10 Scaling of tracheal system and relative visceral trachea length in studied developmental stages of *Tenebrio molitor*. (A) Scaling of tracheal system volume with body tissues volume. Lines represent result of SMA (standardised major axis) calculated separately for two pairs of developmental stages larva–pupa (solid line) and pupa–imago (dotted line). Numbers near lines indicate scaling coefficient of tracheal system. (B) Relative length of visceral tracheae to body length originating from particular spiracles in analysed developmental stages. Boxplots visualize median, upper and lower quartile, greatest and lowest value excluding outliers. as₁–as₈, abdominal spiracles 1–8; ts₁, mesothorax spiracle; ts₂, metathorax spiracle.

systems should be treated as modular units of evolutionary transformation. A modular arrangement of the tracheal system can lead to higher rates of evolvability (Yang, 2001; Lehoux & Cloutier, 2015; Londe et al. 2015), as modular units enable changes of certain body parts without interfering with the functions of the other parts (Wagner, 1996; Klingenberg, 2002, 2009; Sharma et al. 2016). Moreover, it is hypothesised that this phenomenon contributes to optimisation of the whole network by lowering connection costs compared with non-modular builds (Clune et al. 2013) and a high rate of co-option of modules (Monteiro & Podlaha, 2009). During metamorphosis, selected modules undergo various changes (i.e. development/reduction of structural complexity/volume) and in some cases particular units can create higher grade groups, which have the same purpose (e.g. metathoracic modules co-operate to aerate the flight muscle complex) (Fig. 8). Integrations between modules were more developed bilaterally in the antero-posterior axis than in the transverse axis, mainly because of relatively wide longitudinal tracheal trunks (*dlt*, *vlt*).

Serial homologues

Under Hox RNA interference conditions, Ohde et al. (2013) identified dorsolateral denticular outgrowths on the pupal

abdomen of *T. molitor* as wing serial homologues. Tracheae aerating these structures were identified here. By comparison with the tracheal arrangement of metathoracic modules they were recognised as serial homologues of wing and leg tracheae (*rlt*, *rvt*) (Fig. 7D). Furthermore, tracheae with the same structure and relative location were also identified in abdominal modules of other developmental stages (i.e. larvae and adults). The presence of these tracheae supports the assumption of the uniformity of the above-designated tracheal modules (Fig. 6C) and is compatible with observations of developmental potential of different appendages (e.g. wings) on the abdomen under specific genetic conditions (Lewis et al. 2000). Serial homologues of wing and leg trachea can be interpreted as rudimentary, remaining adapted from the common hexapoda ancestor, which has been proved to possess lateral outgrowths on the thorax and the first eight abdominal segments (Kukalová-Peck, 1983; Haug et al. 2015). However, future studies of different species are required to test this hypothesis. The basal connection of wing and leg trachea and their serial homologues can be seen to support the dual origin of insect wing hypothesis proposed by Clark-Hachtel et al. (2013), in which some parts of notum (paranotal lobes) and ancestral exite merge into one functional appendage. From the methodological perspective, the

concept of a tracheal module seems to be a reliable reference for future comparative studies.

Growth rate of tracheal system during metamorphosis

The scaling coefficient is widely used as an indicator for growth patterns of specific systems in relation to body mass or volume (Kaiser et al. 2007; Klingenberg, 2009). Until now, this type of analysis for the whole tracheal system had been performed for only two insect species (Lease et al. 2006; Callier & Nijhout, 2011): the hemimetabolous *Schistocera americana* (Orthoptera) and the larval stages of the holometabolous *Manduca sexta* (Lepidoptera). Investigation of the scaling exponent for all developmental stages of the *T. molitor* tracheal system in a single analysis was methodologically challenging because of the decrease in body volume occurring between pupal and adult stages (Fig. 10A, Table 2). To overcome this obstacle, the obtained data were divided into two separate sets (larva–pupa and pupa–imago) which enabled the calculation of the scaling factor separately for each transition. The scaling pattern of the tracheal system and body volume for the larva–pupa transition is isometric, whereas a positive allometry was registered for the pupa–imago transition. Results obtained for the first transition are consistent with the ones provided by Callier & Nijhout (2011), who studied the tracheal system of *M. sexta* larvae from the second to the fifth instar (mass-scaling coefficient 1.04). On the other hand, in hemimetabolous insects, the tracheal system grew hypermetrically compared with the body mass (mass-scaling coefficient 1.3) (Lease et al. 2006). This trend also occurred in *T. molitor* between pupa and imago but it reached a higher value (Fig. 10A). In conclusion, the development of the body volume is linear in hemimetabolous insects, whereas in holometabola the occurrence of the pupal stage causes a decrease of body volume in the imago. Moreover, changes in the complexity of the structure have been noted by comparison of the fractal dimension index, which was the highest for the imaginal stage and statistically different from the larva and pupa (Table 2). The last ecdysis can be considered to be the most significant in ontogenetic development from the point of view of the tracheal system. The most drastic changes are introduced in the prepupa–pupa stage. The role of the pupal stage in the tracheal system metamorphosis is also highlighted in the number of qualitative changes observed in the locomotory organs (see Chapman, 1918), e.g. reduction of the number of distal wing tracheae (from six to one) in the hind wings of adults (Fig. 2A,B).

Noticeable changes of trachea

The number of the trachea aerating the middle pair of legs seems to vary among Coleoptera. Chapman (1918) stated that in the case of *Monochamus* sp. (Cerambycidae) a single

mesoleg is penetrated by a branching trachea, while in *T. molitor* the meso- and metalegs are aerated by two tracheae (*mplt*, *malt*) that connect to form a common leg trachea (*clt*) before entering the leg. The latter image was also observed by Hafeez & Gardiner (1964) in a relatively close relative of *T. molitor*, *Tribolium anaphe*. Material analysed suggests that at the time of metamorphosis, the differentiation of *mplt* and *malt* occurs in the meso- and metalegs (Figs 2C and 7B). The main role of gas transfer seems to be directed to *malt*, which is shorter and has a larger diameter than the corresponding *mplt* (Fig. 2C). These changes are connected with a modification in the mutual position of legs and spiracles, i.e. legs change their relative location through metamorphosis from between subsequent spiracles (ts_1 – ts_2 , ts_2 – as_1) to posterior spiracle (ts_2 , as_1), from which the *malt* sprouts (Fig. 2C). Development of visceral trachea during metamorphosis is probably linked to the requirements of the developing flight muscles (Figs 1A and 9). The second thoracic and the first abdominal spiracles are devoted to supporting the high demand for respiratory gases during flight (Crowson, 1981; Lehmann & Schutzner, 2010; Snelling et al. 2011). Because of that role, these spiracles lose or reduce visceral tracheae. In response, spiracles of the subsequent abdominal segments take over the function of alimentary canal aeration in the mesothorax and metathorax (Fig. 8).

Conclusion

The structure of the tracheal system is composed of spiracle-oriented modules, which undergo changes during metamorphosis reflecting the development of other systems and tissues. Although 20 different tracheal modules (10 pairs) are present in the body of *T. molitor*, they can be grouped into the three following types on the basis of their unique structure, functionality and development: cephalo-prothoracic (spiracles ts_1), metathoracic (ttv_2 , as_1) and abdominal (as_2 – as_8).

During metamorphosis, the main topological modifications concern tracheae penetrating the middle and hind legs, and aerating muscles of the flight apparatus. Moreover, elongation of the visceral trachea which penetrate the thorax and the abdomen should be treated as a tendency for separation of the tracheal system of the gut from the flight apparatus system.

Additionally, several quantitative changes were reported through metamorphosis, i.e. relative distances between spiracles, number of tracheal ramifications, maximal diameter of tracheae, and dramatic (almost two-fold) volume increase of the whole tracheal system. Most of these modifications occur during the pupal stage, e.g. development of flight muscle tracheae. Development of specific modules leads to formation of higher grade complexes of tracheae connected to specific tissues. Such organ–trachea complexes are most visible in the metathorax, where the metathoracic

and the first abdominal spiracle form an exceptionally developed complex of flight muscles.

Acknowledgements

We thank the Editor and the assigned reviewers for their constructive comments, which helped us to improve the manuscript, and Maxwell V. L. Barclay (Natural History Museum, London) for checking the English language.

This research was funded by the Preludium 12 Project (Number 2016/23/N/NZ8/02815) from the National Science Centre, Poland.

Author contributions

Conceptualisation: D.I.. Formal analysis: M.R.. Investigation: M.R.. Methodology: M.R., D.I., M.J.K.. Software: M.R., M.J.K.. Supervision: D.I., M.J.K.. Visualization: M.R.. Writing – original draft: M.R., M.J.K.. Writing – review & editing: M.R., D.I., M.J.K.

References

- Affolter M, Shilo B-Z (2000) Genetic control of branching morphogenesis during *Drosophila* tracheal development. *Curr Opin Cell Biol* **12**, 731–735.
- Beutel RG, Komarek A (2004) Comparative study of thoracic structures of adults of Hydrophiloidea and Histeroidea with phylogenetic implications (Coleoptera, Polyphaga). *Org Divers Evol* **4**, 1–34.
- Beutel RG, Pohl H (2006) Endopterygota systematics – where do we stand and what is the goal (Hexapoda, Arthropoda)? *Syst Entomol* **31**, 202–219.
- Bradley TJ, Briscoe AD, Brady SG, et al. (2009) Episodes in insect evolution. *Integr Comp Biol* **49**, 590–606.
- Callier V, Nijhout HF (2011) Control of body size by oxygen supply reveals size-dependent and size-independent mechanisms of molting and metamorphosis. *PNAS* **108**, 14664–14669.
- Casanova J (2007) The emergence of shape: notions from the study of the *Drosophila* tracheal system. *EMBO Rep* **8**, 335–339.
- Centanin L, Gorr TA, Wappner P (2010) Tracheal remodelling in response to hypoxia. *J Insect Physiol* **56**, 447–454.
- Chapman RN (1918) *The Basal Connection of the Trachea of the Wing*. Ithaca, NY: The Comstock Publishing Company, pp. 28–51.
- Clark-Hachtel CM, Linz DM, Tomoyasu Y (2013) Insights into insect wing origin provided by functional analysis of vestigial in the red flour beetle, *Tribolium castaneum*. *PNAS* **110**, 16951–16956.
- Clune J, Mouret J-B, Lipson H (2013) The evolutionary origins of modularity. *Proc R Soc B* **280**, 20122863.
- Conteras HL, Bradley TJ (2010) Transitions in insect respiratory patterns are controlled by changes in metabolic rate. *J Insect Physiol* **56**, 522–528.
- Crowson RA (1955) *The Natural Classification of the Families of Coleoptera*. London: N. Lloyd, pp. 187.
- Crowson RA (1981) *The Biology of the Coleoptera*. London: Academic Press, pp. 802.
- Doyen JT (1966) The skeletal anatomy of *Tenebrio molitor* (Coleoptera: Tenebrionidae). *Misc Publ Entomol Soc Am* **5**, 103–150.
- Duncan FD, Forster TD, Hetz SK (2010) Pump out the volume – the effect of tracheal and subelytral pressure pulses on convective gas exchange in a dung beetle, *Circellium bacchus* (Fabricus). *J Insect Physiol* **56**, 551–558.
- Ebenman B (1992) Evolution in organisms that change their niches during the life cycle. *Am Nat* **139**, 990–1021.
- Ferns PN, Jervis MA (2016) Ordinal species richness in insects – a preliminary study of the influence of morphology, life history, and ecology. *Entomol Exp Appl* **159**, 270–284.
- Ghabrial AS, Levi BP, Krasnow MA (2011) A systematic screen for tube morphogenesis and branching genes in the *Drosophila* tracheal system. *PLoS Genet* **7**, e1002087.
- Gillott C (2005) *Entomology*, 3rd edn. Dordrecht: Springer, pp. 831.
- Given BB (1944) The anatomy of the final larval instar of *Diodromus* (*Thyraeella*) *collaris* Grav. (Ichneumonidae), with notes on structural changes through the prepupal and pupal stages. *Trans R Soc N Z* **74**, 297–301.
- Greco M, Bell D, Woolnough L, et al. (2014) 3-D visualisation, printing, and volume determination of the tracheal respiratory system in the adult desert locust, *Schistocerca gregaria*. *Entomol Exp Appl* **152**, 42–51.
- Greenlee KJ, Harrison JF (2005) Respiratory changes throughout ontogeny in the tobacco hornworm caterpillar, *Manduca sexta*. *J Exp Biol* **208**, 1385–1392.
- Greenlee KJ, Henry JR, Kirkton SD, et al. (2009) Synchrotron imaging of the grasshopper tracheal system: morphological and physiological components of tracheal hypermetry. *Am J Physiol Regul Integr Comp Physiol* **297**, R1343–R1350.
- Greenlee KJ, Socha JJ, Eubanks HB, et al. (2013) Hypoxia-induced compression in the tracheal system of the tobacco hornworm caterpillar, *Manduca sexta*. *J Exp Biol* **216**, 2293–2301.
- Grimaldi DA (2010) 400 million years on six legs: on the origin and early evolution of Hexapoda. *Arthropod Struct Dev* **39**, 191–203.
- Grimaldi D, Engel MS (2005) *Evolution of the Insects*. Cambridge: Cambridge University Press, pp. 772.
- Hafeez MA, Gardiner BG (1964) The internal morphology of the adult of *Tribolium anaphe* Hinton (Coleoptera: Tenebrionidae). *Proc R Entomol Soc Lond A Gen Entomol* **39**, 137–145.
- Harrison JF, Lafreniere JJ, Greenlee KJ (2005) Ontogeny of tracheal dimensions and gas exchange capacities in the grasshopper, *Schistocerca americana*. *Comp Biochem Physiol A Mol Integr Physiol* **141**, 372–380.
- Haug JT, Labandeira CC, Santiago-Blay JA, et al. (2015) Life habits, hox genes, and affinities of a 311 million-year-old holometabolous larva. *BMC Evol Biol* **15**, 208.
- Helm BR, Davidowitz G (2013) Mass and volume growth of an insect tracheal system within a single instar. *J Exp Biol* **216**, 4703–4711.
- Hildebrand T, Rügsegger P (1997) Quantification of bone microarchitecture with the structure model index. *Comput Methods Biomech Biomed Engin* **1**, 15–23.
- Iwan D, Kamiński MJ, Raś M (2015) The last breath: a μ CT-based method for investigating the tracheal system in Hexapoda. *Arthropod Struct Dev* **44**, 2018–2227.
- Jögar K, Metspalu L, Hiiesaar K, et al. (2005) Physiology of diapause in pupae of *Pieris brassicae* L. (Lepidoptera: Pieridae). *Agron Res* **3**, 21–37.

- Jorstad A, Nigro B, Cali C, et al. (2014) NeuroMorph: a toolset for the morphometric analysis and visualization of 3D models derived from electron microscopy image stacks. *Neuroinformatics* **13**, 83–92.
- Kaiser A, Klok CJ, Socha JJ, et al. (2007) Increase in tracheal investment with beetle size supports hypothesis of oxygen limitation on insect gigantism. *PNAS* **104**, 13198–13203.
- Keister ML (1948) The morphogenesis of the tracheal system of *Sciara*. *J Morphol* **83**, 373–423.
- Kennedy CH (1922) The homologies of the tracheal branches in the respiratory system of insects. *Ohio J Sci* **XXII**, 84–89.
- Klingenberg CP (2002) Morphometrics and the role of the phenotype in studies of the evolution of developmental mechanisms. *Gene* **287**, 3–10.
- Klingenberg CP (2009) Morphometric integration and modularity in configurations of landmarks: tools for evaluating a priori hypotheses. *Evol Dev* **11**, 405–421.
- Kraus O (1997) Phylogenetic relationships between higher taxa of tracheate arthropods. *Arthropod Relatsh* **55**, 295–303.
- Kukalová-Peck J (1983) Origin of the insect wing and wing articulation from the arthropodan leg. *Can J Zool* **61**, 1618–1669.
- Lawrence J, Hastings A, Dallwitz M, et al. (1994) *Beetle Larvae of the World*. Melbourne: CSIRO Publishing.
- Lawrence JF, Ślipiński A, Seago AE, et al. (2011) Phylogeny of the Coleoptera based on morphological characters of adults and larvae. *Annal Zool* **61**, 1–217.
- Lease HM, Wolf BO, Harrison JF (2006) Intraspecific variation in tracheal volume in the American locust, *Schistocerca americana*, measured by a new inert gas method. *J Exp Biol* **209**, 3476–3483.
- Lehmann F-O, Schutzner P (2010) The respiratory basis of locomotion in *Drosophila*. *J Insect Physiol* **56**, 543–550.
- Lehoux C, Cloutier R (2015) Building blocks of a fish head: developmental and variational modularity in a complex system. *J Exp Zool Mol Dev Evol* **324B**, 614–628.
- Lewis DL, DeCamillis M, Bennett R (2000) Distinct roles of the homeotic genes Ubx and abd-A in beetle embryonic abdominal appendage development. *PNAS* **97**, 4504–4509.
- Li D, Zhu P, Wu Z, et al. (2011) 3D configuration of mandibles and controlling muscles in rove beetles based on micro-CT technique. *Anal Bioanal Chem* **401**, 817–825.
- Locke M (1958) The co-ordination of growth in the tracheal system of insects. *Q J Microsc Sci* **99**, 373–391.
- Londe S, Monnin T, Cornette R, et al. (2015) Phenotypic plasticity and modularity allow for the production of novel mosaic phenotypes in ants. *Evodevo* **6**, 36.
- Long SKR, Fulkerson E, Breese R, et al. (2014) A comparison of midline and tracheal gene regulation during *Drosophila* development. *PLoS ONE* **9**, e85518.
- Loudon C (1989) Tracheal hypertrophy in mealworms: design and plasticity in oxygen supply system. *J Exp Biol* **147**, 217–235.
- Lowe T, Garwood RJ, Simonsen TJ, et al. (2013) Metamorphosis revealed: time-lapse three-dimensional imaging inside a living chrysalis. *J R Soc Interface* **10**, 20130304.
- Maina JN (2002) Structure, function and evolution of the gas exchangers: comparative perspectives. *J Anat* **201**, 281–304.
- May RM (2011) Why worry about how many species and their loss? *PLoS Biol* **9**, e1001130.
- Metzger RJ, Krasnow MA (1999) Genetic control of branching morphogenesis. *Science* **284**, 1635–1639.
- Moerbitz C, Hetz SK (2010) Tradeoffs between metabolic rate and spiracular conductance in discontinuous gas exchange of *Samia cynthia* (Lepidoptera, Saturniidae). *J Insect Physiol* **56**, 536–542.
- Monteiro A, Podlaha O (2009) Wings, horns, and butterfly eye-spots: how do complex traits evolve? *PLoS Biol* **7**, e1000037.
- Mora C, Tittensor DP, Adl S, et al. (2011) How many species are there on earth and in the ocean? *PLoS Biol* **9**, e1001127.
- Morales-Ramos JA, Kay S, Rojas MG, et al. (2015) Morphometric analysis of instar variation in *Tenebrio molitor* (Coleoptera: Tenebrionidae). *Ann Entomol Soc Am* **108**, 146–159.
- Nardi JB, Ujhelyi E (1998) Remodeling of neural, glial, and tracheal cell populations in the developing *Manduca* wing. *Cell Tissue Res* **294**, 367–375.
- Nespolo RF, Sepúlveda RD, Castañeda LE, et al. (2011) Effects of shape variations on the energy metabolism of the sand cricket *Gryllus firmus*: a geometric morphometric analysis. *Biol Res* **44**, 69–74.
- Nicholson DB, Ross AJ, Mayhew PJ (2014) Fossil evidence for key innovations in the evolution of insect diversity. *Proc R Soc B* **281**, 20141823.
- Ohde T, Yaginuma T, Niimi T (2013) Insect morphological diversification through the modification of wing serial homologs. *Science* **340**, 495.
- Packard AS (1898) *Text-Book of Entomology*. New York: The Macmillan Company, pp.729.
- Pereanu W, Spindler S, Cruz L, et al. (2007) Tracheal development in the *Drosophila* brain is constrained by glial cells. *Dev Biol* **302**, 169–180.
- Pick C, Schneuer M, Burmester T (2009) The occurrence of hemocyanin in Hexapoda. *FEBS J* **276**, 1930–1941.
- Pitsouli C, Perrimon N (2010) Embryonic multipotent progenitors remodel the *Drosophila* airways during metamorphosis. *Development* **137**, 3615–3624.
- R Core Team (2013) *R: A Language and Environment for Statistical Computing*. Vienna: R Foundation for Statistical Computing. ISBN 3-900051-07-0, URL: <http://www.R-project.org>
- Raś M (2017) Tracheal system in post-embryonic development of holometabolous insects: a case study using mealworm beetle. <https://doi.org/10.7910/dvn/5cgmth>, Harvard Dataverse, V2, UNF:6:BUHGWWV7TOxKoBVYTvpaZkQ==
- Richards OW, Davies RG (1977) Chapter 13: The respiratory system. In: *IMMS' General Textbook of Entomology*, 10th edn (eds Richards OW, Davies RG), pp. 209–233. London: Chapman and Hall.
- Romer F (1971) Die Prothorakaldrüsen der Larve von *Tenebrio molitor* L. (Tenebrionidae, Coleoptera) und ihre Veränderungen während eines Hautungszyklus. *Z Zellforsch* **122**, 425–455.
- Scott GG (1905) The distribution of trachea in the nymph of *Platthemis lydia*. *Biol Bull* **IX**, 341–354.
- Sharma AI, Yanes KO, Jin L, et al. (2016) The phenotypic plasticity of developmental modules. *Evodevo* **7**, 15.
- SkyScan (2005) *Instruction Manual, Skyscan 1172 Desktop Micro-CT*. Belgium: Skyscan, pp. 54.
- Sláma K, Jedlička P (2012) Respiratory metabolism of the pea aphid, *Acyrtosiphon pisum* (Hemiptera: Aphididae). *Eur J Anatol* **109**, 491–502.
- Smith DB, Bernhardt G, Raine NE, et al. (2016) Exploring miniature insect brains using micro-CT scanning techniques. *Sci Rep* **6**, 21768.
- Snelling EP, Seymour RS, Runciman S, et al. (2011) Symmorphosis and the insect respiratory system: allometric variation. *J Exp Biol* **214**, 3225–3237.

- Snodgrass RE** (1910) *The Anatomy of the Honey Bee*. Technical Series U.S. Department of Agriculture, 18: 1–116.
- Snodgrass RE** (1935) *Principles of Insect Morphology*. New York: McGraw-Hill Book Company, Inc., pp. 667.
- Socha JJ, Lee W-K, Harrison JF, et al.** (2008) Correlated patterns of tracheal compression and convective gas exchange in a carabid beetle. *J Exp Biol* **211**, 3409–3420.
- Socha JJ, Förster TD, Greenlee KJ** (2010) Issues of convection in insect respiration: insights from synchrotron X-ray imaging and beyond. *Respir Physiol Neurobiol* **173S**, S65–S73.
- Sokal RR, Rohlf FJ** (2011) *Biometry*. San Francisco: W.H. Freeman, pp. 937.
- Srivastava KP** (1975) On the respiratory system of the lemon-butterfly, *Papilio demoleus* L. (LEPIDOPTERA PAPILIONIDAE). *J Aust Entomol Soc* **14**, 363–370.
- Sutherland D, Samakovlis C, Krasnow MA** (1996) *branchless* Encodes a *Drosophila* FGF homolog that controls tracheal cell migration and the pattern of branching. *Cell* **87**, 1091–1101.
- Szwanwicz B** (1956) *Entomologia Ogólna*. Warsaw: Państwowe wydawnictwo Rolnicze i Leśne, pp. 991.
- Tonapi GT** (1977) Some adaptative features in the respiratory system of *Dineutes indicus* Aubé (Coleoptera, Gyrinidae). *Zoolog Scr* **6**, 107–112.
- Ureña E, Chafino S, Manjón C, et al.** (2016) The occurrence of the holometabolous pupal stage requires the interaction between E93, Krüppel-homolog 1 and broad-complex. *PLoS Genet* **12**, e1006020.
- Wagner GP** (1996) Homologues, natural kinds and the evolution of modularity. *Am Zool* **36**, 36–43.
- Walker SM, Schwyn DA, Mokso R, et al.** (2014) In vivo time-resolved microtomography reveals the mechanics of the blowfly flight motor. *PLoS Biol* **12**, e1001823.
- Warton DI, Duursma RA, Falster DS, et al.** (2012) SMATR 3 – an R package for estimation and inference about allometric lines. *Methods Ecol Evol* **3**, 257–259.
- Waters JS, Lee W-K, Westneat MW, et al.** (2013) Dynamics of tracheal compression in the horned passalus beetle. *Am J Physiol Regul Integr Comp Physiol* **304**, R621–R627.
- Westneat MW, Socha JJ, Lee E-K** (2008) Advances in biological structure, function, and physiology using synchrotron X-ray imaging. *Annu Rev Physiol* **70**, 119–142.
- Whitten JM** (1957) The post-embryonic development of the tracheal system in *Drosophila melanogaster*. *Q J Microsc Sci* **98**, 123–150.
- Whitten JM** (1968) Metamorphic changes in insects. In: *Metamorphosis a Problem in Developmental Biology* (eds Etkin W, Gilbert LI), pp. 43–105. Amsterdam: North-Holland Publishing Company.
- Wickham H** (2009) *ggplot2: Elegant Graphics for Data Analysis (Use R!)*. New York: Springer, pp. 213.
- Wigglesworth VB** (1954) Growth and regeneration in the tracheal system of an insect, *Rhodinus prolixus* (Hemiptera). *Q J Microsc Sci* **95**, 115–137.
- Yang AS** (2001) Modularity, evolvability, and adaptive radiations: a comparison of the hemi- and holometabolous insects. *Evol Dev* **3**, 59–72.